Half-Heusler semiconductors as piezoelectrics

Anindya Roy, Joseph W. Bennett, Karin M. Rabe* and David Vanderbilt
Department of Physics and Astronomy
Rutgers University, Piscataway, NJ 08854
** Corresponding Author: rabe@physics.rutgers.edu*

(Dated: July 27, 2011)

One of the central challenges in materials science is the design of functional and multifunctional materials, in which large responses are produced by applied fields and stresses. A rapidly developing paradigm for the rational design of such materials is based on the first-principles study of a large materials family, the perovskite oxides being the prototypical case. Specifically, first-principles calculations of structure and properties are used to explore the microscopic origins of the functional properties of interest and to search a large space of equilibrium and metastable phases to identify promising candidate systems. In this paper, we use a first-principles rational-design approach to demonstrate semiconducting half-Heusler compounds as a previously-unrecognized class of piezoelectric materials, and to provide guidance for the experimental realization and further investigation of high-performance materials suitable for practical applications.

The *ABC* half-Heusler compounds (with MgAgAs structure type, also called semi-Heusler or Juza-Nowotny compounds [1]) are a large and varied family, with almost 150 distinct *ABC* half-Heusler compounds reported in the *Inorganic Crystal Structural Database* (ICSD) [2]. The half-Heusler structure, shown in Fig. 1, has $F\bar{4}3m$ symmetry and can be viewed as a rocksalt lattice formed from two of the three constituent atoms (at Wyckoff positions 4a and 4b), with the third atom filling half of the tetrahedral interstitial sites (either Wyckoff position 4c or 4d); it is related to the A_2BC Heusler structure by removal of one of the *A* sublattices, and can alternately be viewed as a stuffed *AC* or *BC* zincblende structure [3].

Following an initial wave of interest stimulated by the observation of half-metallic ferromagnetic behavior in half-Heusler compounds [4], there has been a resurgence of interest in these compounds as materials that can display topological properties [5, 6] or be tailored for uses as diverse as components in spintronic devices [7] and high-performance thermoelectrics [8–10]. The half-Heusler family is regarded as especially versatile as it displays a wide range of functionality, lattice constants, and band gaps.

The semiconducting half-Heusler compounds are of particular interest. True gaps on the order of 1 eV were predicted in Li-containing half-Heusler intermetallic compounds in first-principles calculations by Wood *et al.* [11] in 1985. The most well-studied of these compounds include LiMg*X* and LiZn*X* (where *X*=N, P and As), LiMgSb, and the cell-doubled compounds Li_3AlN_2, Li_3GaN_2, and Li_3GaP_2. Since the identification of NiSnZr as a semiconducting half-Heusler compound through a combination of experimental observations and first-principles investigations [12, 13], many additional semiconducting systems have been identified [3, 14, 15]. Some of these compounds, such as LiMgN and LiMgP, have quite substantial gaps that may make them suitable for solar cell applications [16–18].

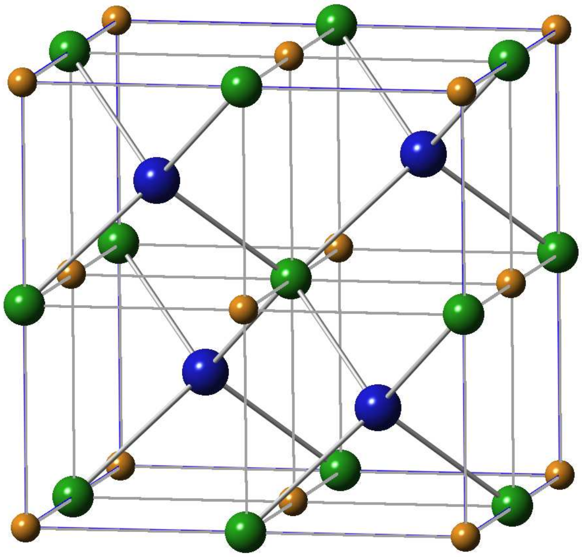

FIG. 1: The *ABC* half-Heusler structure type: *A* (green) and *B* (orange) are arranged in a rocksalt lattice, with the tetrahedral coordination of *C* (blue) by *A* shown.

As insulators, the semiconducting half-Heuslers can also exhibit functional properties associated with electric polarization, but these properties have received very little attention. In fact, while the $F\bar{4}3m$ space group of the half-Heusler structure allows a nonzero d_{14} piezoelectric response, no measurements of piezoelectricity in these systems have yet been reported in the literature.

In this paper, we use first-principles methods to predict the piezoelectric response and related properties of half-Heusler compounds. We present these predictions first for compounds already reported in the half-Heusler structure. We then perform a high-throughput analysis of a much larger set of candidate combinations, identifying high-performance compounds for practical application. Through targeted synthesis, which might include compositional substitution, epitaxial growth or artificial structuring, half-Heusler compounds could thus be developed as a valuable class of piezoelectric materials.

First-principles calculations are performed with the ABINIT package [19–21] using the local density approximation (LDA) and an 8×8×8 Monkhorst-Pack sampling of the fcc Brillouin zone [22]. Norm-conserving Troullier-Martins pseudopotentials are employed, with a plane-wave cutoff of 30 Ha. For selected compounds, the results were verified using optimized norm-conserving pseudopotentials [23, 24] generated using the OPIUM code [25].

For the high-throughput search, we consider combinations of three distinct elements ABC. We limit the search to combinations with a total of 8 s and p valence electrons, since we expect this to improve the likelihood of band gap formation [3]. We also require that there be at least one and at most two p-block elements among the three constituents, with the remainder coming from the s and/or d blocks of the periodic table. We use Roman numerals to denote the valences of the constituent elements (including d electrons) to classify the combinations into families with 8 valence electrons (I-I-VI, I-II-V, I-III-IV, II-II-IV, and II-III-III), 18 valence electrons (XI-I-VI, XI-II-V, XI-III-IV, I-XII-V, II-XII-IV, III-XII-III, X-II-VI, X-III-V, and X-IV-IV), or 28 valence electrons (X-XII-VI, XI-XI-VI, XI-XII-V and XII-XII-IV). Among these families, we consider members constructed from the selections I=(Li, Na), II=(Be, Mg, Ca, Sr, Ba), III=(B, Sc, Y, Al, Ga), IV=(C, Si, Ge, Sn, Pb, Ti, Zr, Hf), V=(N, P, As, Sb, Bi), VI=(O, S, Se, Te), X=(Ni, Pd, Pt), XI=(Cu, Ag, Au), and XII=(Zn, Cd). This generates a total of 792 candidate combinations to be searched.

We first consider the 36 combinations in our search set that have been experimentally reported in the ICSD. For each combination, we optimize the lattice constant for each of the three structural variants $\underline{A}BC$, $A\underline{B}C$, and $AB\underline{C}$, where the underscore indicates the unique element that is tetrahedrally coordinated by both of the two other elements. First-principles results show that 23 of them, listed in Table I, are insulating. The predicted lowest-energy structural variant is indicated in the first column. We find that for the five compounds (LiZnAs, AuScSn, NiScSb, PdScSb and PtYSb) for which a refined structure, including R value and temperature factors, is available in ICSD, our prediction agrees with the experimentally observed variant. Most of the computed equilibrium lattice constants given in Table I are in excellent agreement with experiment. The computed gaps range from 0.15 eV for NiScBi to 1.42 eV for PtZrSn.

For each compound, we perform a linear-response calculation using density-functional perturbation theory (DFPT) [26], as implemented in ABINIT, to compute the dynamical charges and zone-center phonon frequencies and eigenvectors, from which the free-stress static dielectric constant ϵ_0 can be obtained [27].

ABC	$a_{\rm expt.}$	a	$E_{\rm gap}$	d_{14}	C_{44}	k_{14}	ϵ_0
	(Å)	(Å)	(eV)	(pC/N)	(10^{11}Pa)		
LiMg$\underline{\text{P}}$	6.02	5.94	1.38	3.2	0.46	0.07	11.33
LiMg$\underline{\text{As}}$	6.19	6.10	1.15	2.2	0.41	0.04	12.61
LiMg$\underline{\text{Bi}}$	6.74	6.52	0.69	0.3	0.31	0.00	15.76
LiZn$\underline{\text{N}}$	4.87	4.85	0.72	7.6	0.82	0.18	15.39
LiZn$\underline{\text{P}}$	5.78	5.64	1.11	12.1	0.57	0.24	15.92
LiZn$\underline{\text{As}}$	5.94	5.81	0.61	13.5	0.58	0.24	20.08
LiCd$\underline{\text{P}}$	6.09	6.02	0.51	0.4	0.44	0.01	19.18
$\underline{\text{Au}}$ScSn	6.42	6.41	0.22	10.2	0.56	0.17	22.57
$\underline{\text{Ni}}$TiSn	5.94	5.82	0.50	0.2	0.90	0.00	29.04
$\underline{\text{Ni}}$ZrSn	6.11	6.13	0.60	13.7	0.67	0.22	28.38
$\underline{\text{Ni}}$HfSn	6.08	6.06	0.52	10.9	0.79	0.19	28.38
$\underline{\text{Pd}}$ZrSn	6.32	6.35	0.56	13.1	0.61	0.21	25.02
$\underline{\text{Pd}}$HfSn	6.30	6.29	0.51	10.8	0.71	0.19	24.71
$\underline{\text{Pt}}$TiSn	6.16	6.08	1.09	0.7	0.94	0.02	21.92
$\underline{\text{Pt}}$ZrSn	6.32	6.35	1.42	9.3	0.74	0.19	20.00
$\underline{\text{Pt}}$HfSn	6.31	6.29	1.40	7.3	0.85	0.16	19.28
$\underline{\text{Ni}}$ScSb	6.06	6.04	0.30	12.6	0.70	0.23	22.96
$\underline{\text{Ni}}$ScBi	6.19	6.30	0.15	4.1	0.57	0.06	27.99
$\underline{\text{Ni}}$YSb	6.31	6.43	0.28	242.3	0.05	0.77	23.30
$\underline{\text{Pd}}$ScSb	6.31	6.29	0.31	10.9	0.59	0.19	21.12
$\underline{\text{Pd}}$YSb	6.53	6.63	0.19	33.0	0.25	0.35	21.81
$\underline{\text{Pt}}$ScSb	6.31	6.27	1.04	9.9	0.72	0.19	20.31
$\underline{\text{Pt}}$YSb	6.54	6.59	0.34	58.2	0.21	0.50	24.50

TABLE I: Properties of experimentally synthesized half-Heuslers, grouped by family. Experimental lattice constants are from the ICSD. Also presented are the theoretical lattice constant a, band gap $E_{\rm gap}$, piezoelectric coefficient d_{14}, electromechanical coupling coefficient k_{14}, and free-stress static dielectric constant ϵ_0.

We also carry out calculations of the strain response [28, 29] to obtain the C_{44} elastic constant and d_{14} piezoelectric coefficient. All this information can be combined to obtain the electromechanical coupling coefficient k_{14} as described in Ref. 28 using the formula $k_{14} = |d_{14}|\sqrt{C_{44}/(\epsilon_{\rm fs}\epsilon_0)}$, where $\epsilon_{\rm fs}$ is the permittivity of free space, and ϵ_0 is our computed dimensionless free-stress dielectric constant.

The results are included in Table I. The computed values of the piezoelectric constant d_{14} mostly fall in the range from 2.0 to 14 pC/N. All but five compounds have $d_{14} > 2.6$ pC/N, the experimentally measured piezoelectric coefficient of GaAs. The highest values found are for NiYSb, PdYSb and PtYSb, and can be associated with their small bandgap, large ϵ_0 and low elastic constant. These three compounds also have the highest values of electromechanical coupling k_{14}, as shown in Table I, arising from their large d_{14} and low elastic constant, though limited by the size of ϵ_0.

It is remarkable that no piezoelectric response data for any half-Heusler compound has yet been reported. With a single-crystal sample of sufficiently low conductivity,

---

[1] The thirteen metallic combinations are LiAlSi, LiGaSi, LiAlGe, BeAlB, CuMgSb, AgMgAs, CuMgBi, AuCaBi, NiYBi, CuCdSb, AgCdSb, AuCdSb, and AuYPb.

the piezoelectric coefficient should be readily measurable for most if not all of these compounds. Moreover, measurements of the dielectric response and elastic coefficients, which also have not been reported to date, would provide an additional test of these theoretical predictions and a more complete characterization of the polarization-related properties of these otherwise much-studied compounds.

Next, we consider the properties of the full set of 792 hypothetical and real ABC combinations identified earlier for study. As before, for each combination we optimize the lattice constant for each of the variants $\underline{A}BC$, $A\underline{B}C$, and $AB\underline{C}$. Choosing the variant having the lowest total energy, we determine whether our LDA calculations predict it to be insulating. Of the 792 combinations, we find 234 insulators having either 8 or 18 valence electrons, while the compounds containing 28 valence electrons are all found to be metallic. For the insulators, we perform linear-response calculations using ABINIT as described above, except that we also compute the C_{11} and C_{12} elastic constants. This allows us to screen for local elastic stability by requiring that the elastic constants satisfy $C_{11} + 2C_{12} > 0$, $C_{44} > 0$, $C_{11} - C_{12} > 0$, as described in Ref. 30 and references therein. Furthermore, we calculate phonon frequencies at three additional high-symmetry points (X, L and W) and eliminate combinations which exhibit any unstable modes. This reduces the combinations further from 234 down to 189.

We thus arrive at 189 combinations that are predicted to be insulating and locally stable in the lowest-energy variant of the three possible ABC half-Heusler structures. Since DFT tends to underestimate band gaps, we expect that the actual fraction of insulating structures will be slightly higher than our calculations would indicate. The computed band gaps and lattice parameters for these 189 compounds are shown in Figure 2. We expected no particular correlation between lattice parameter and band gap, and indeed we find none. Both quantities are rather broadly distributed, suggesting that there could be considerable flexibility in choosing materials over a substantial range of desired gap or lattice constant.

For these 189 compounds, we also compute d_{14}, k_{14}, and ϵ_0 using the same methods as before. To give a sense of how the range of properties in the full set of known and hypothetical compounds compares with that of the subset of known compounds, we present a scatter plot of k_{14} vs log d_{14} in Figure 3.

It can be seen that there are hypothetical compounds with k_{14} and d_{14} values well above those of known compounds (some have k_{14} close to one and d_{14} up to several hundred). We also find that these two quantities show the expected positive correlation. The twelve compounds with the highest values of d_{14} are listed in Table II. As d_{14} is determined both by the polarization-strain response e_{14} and the shear elastic constant, large values can arise either from the former being large, the latter being small, or both; this is reflected in the examples in Table II, where all C_{44} are small.

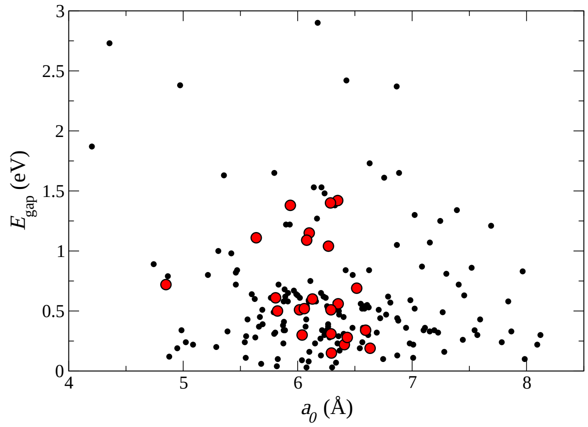

FIG. 2: Cell parameters (in Å) of insulating ABC combinations as well as their range of band gaps (in eV) are depicted as open black circles. Known combinations, from Table 1, are highlighted as filled red circles

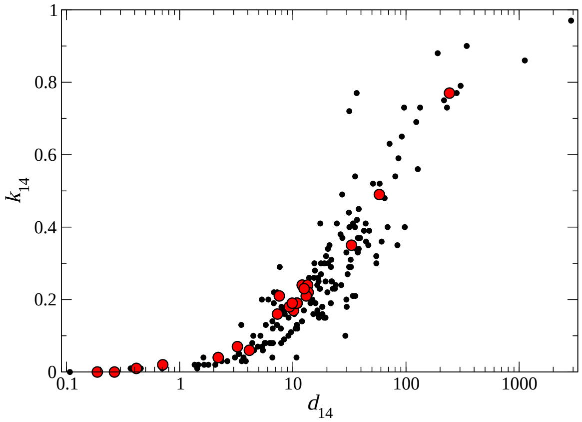

FIG. 3: Electromechanical coupling factor k_{14} of insulating ABC combinations as a function of piezoelectric constant d_{14}. Known combinations, from Table 1, are highlighted as filled red circles

ABC	a (Å)	E_{gap} (eV)	d_{14} (pC/N)	C_{44} (10^{11}Pa)	k_{14}	ϵ_0
SrCd$\underline{\text{Si}}$	7.01	0.11	2878.8	0.01	0.97	24.98
SrAl$\underline{\text{Ga}}$	6.87	0.13	1122.3	0.01	0.86	48.85
NaZn$\underline{\text{P}}$	6.07	0.37	344.1	0.06	0.90	17.79
Na$\underline{\text{B}}$Ge	5.56	0.43	304.2	0.03	0.79	18.12
MgSr$\underline{\text{Si}}$	7.09	0.87	280.4	0.04	0.80	20.63
$\underline{\text{Ni}}$YSb	6.43	0.28	242.3	0.05	0.77	23.30
MgSr$\underline{\text{Ge}}$	7.11	0.36	230.4	0.05	0.75	21.95
CuY$\underline{\text{Si}}$	6.36	0.50	217.0	0.05	0.76	19.87
NaMg$\underline{\text{N}}$	5.46	0.72	190.6	0.09	0.87	11.33
BeSc$\underline{\text{B}}$	5.39	0.33	133.4	0.13	0.72	23.84
MgSr$\underline{\text{Sn}}$	7.41	0.72	127.2	0.07	0.58	25.56
LiCa$\underline{\text{P}}$	6.63	1.73	123.2	0.07	0.72	10.82

TABLE II: Top twelve half-Heusler compounds, ranked according to piezoelectric coefficient d_{14}.

ABC	a (Å)	E_{gap} (eV)	d_{14} (pC/N)	C_{44} (10^{11}Pa)	k_{14}	ϵ_0
LiY$\underline{\text{C}}$	5.83	0.72	58.5	0.17	0.52	17.54
CuY$\underline{\text{Ge}}$	6.36	0.47	55.3	0.19	0.49	20.18
AgY$\underline{\text{Si}}$	6.55	0.56	47.3	0.14	0.40	18.79
MgCa$\underline{\text{Si}}$	6.79	0.62	44.0	0.19	0.43	18.17
MgCa$\underline{\text{Ge}}$	6.81	0.57	42.6	0.19	0.41	19.25
NaSc$\underline{\text{C}}$	5.77	0.61	38.2	0.32	0.44	21.12
LiY$\underline{\text{Si}}$	6.58	0.54	38.2	0.17	0.35	19.91
LiY$\underline{\text{Ge}}$	6.58	0.52	37.5	0.17	0.34	20.41
ZnSc$\underline{\text{B}}$	5.63	0.28	36.9	0.32	0.41	23.70
AgY$\underline{\text{Ge}}$	6.56	0.52	36.2	0.17	0.34	19.35
MgZn$\underline{\text{C}}$	5.22	0.80	35.5	0.50	0.51	20.14
NaAl$\underline{\text{Si}}$	6.26	0.34	35.4	0.27	0.41	19.25
$\underline{\text{Ni}}$ScP	5.79	0.49	34.1	0.30	0.41	19.75
CaSr$\underline{\text{Ge}}$	7.57	0.30	33.9	0.12	0.25	24.27
MgCa$\underline{\text{Sn}}$	7.10	0.34	32.6	0.19	0.31	21.78

TABLE III: Best fifteen remaining half-Heusler compounds, ranked according to piezoelectric coefficient d_{14}. None of the initial top twelve presented in Table II remain after considering band gap, stability, cost and toxicity.

As a guide for experimental investigation of piezoelectric half-Heusler compounds, we also present an alternative selection of compounds chosen according to relevant practical considerations. We filter the list to eliminate compounds with toxic (Pb, Cd, As) or expensive (Be, Pd, Pt) elements. In addition, we require a DFT band gap above $0.4\,\text{eV}$ to favor low sample conductivity. Lastly, to promote cation ordering into the lowest-energy variant, we require $\Delta E > 0.15\,\text{eV}$, where ΔE is the difference in energy between the lowest-energy and next-lowest-energy variants. Of the remaining 65 compounds that satisfy these criteria, 59 have $d_{14} > 2.6\,\text{pC/N}$, the experimental value of GaAs. The fifteen with the largest d_{14} values are presented in Table III.

Further investigation of the hypothetical half-Heusler piezoelectrics hinges on the possibility of experimentally realizing the desired compounds in the half-Heusler structure. Additional information about bulk equilibrium ABC phases can be obtained from the ICSD. In the cases where no phase is reported, it could be that either no stable bulk phase exists with that stoichiometry, or simply that the relevant composition has not been studied. ABC combinations are also reported in several structures other than the half-Heusler structure. Specifically, we find that nine combinations listed in Table III are reported in the ICSD with other structures: MgSrSi, MgCaSi and MgCaGe are reported with structures in the $Pnma$ space group, while NaBaP, AgYSi and LiYSi are reported to have structures with $P\bar{6}2m$ symmetry. The latter space group is piezoelectric, so these compounds can offer an additional route to new piezoelectrics. Moreover, 13 compounds of the original 792 combinations are reported in two different space groups, namely LiMgN, LiSrP, LiBaP, LiAlGe, CuMgAs, AgCaBi, CuScSn, CuYSn, AuScSn, CaZnSn, PdTiGe, NaAgO and LiAuS. Of these, only AuScSn is reported in the half-Heusler structure, while none are found in either Tables II or III.

This structural variety should encourage interest in further exploration of these systems for piezoelectricity and other functional behavior. Polymorphism suggests the possibility of intentionally stabilizing one of several competing structures, or of switching between them at will, via the application of external stresses, fields, or other perturbations.

First-principles calculations of the total energy of alternative structures could be used both to predict ground state structures and to identify systems with piezoelectric structures as low-energy alternatives that would be suitable candidates for stabilization through compositional substitution or epitaxial strain. Furthermore, half-Heusler systems offer the opportunity to combine piezoelectricity with other functional properties, including magnetism, to produce multifunctional behavior of fundamental scientific interest and for groundbreaking technological applications.

In summary, we have used a first-principles rational-design approach to demonstrate semiconducting half-Heusler compounds as a previously unrecognized class of piezoelectric materials. We have presented these predictions first for compounds already reported in the half-Heusler structure, and then for a much larger set of candidate combinations that were generated and screened for high performance via a high-throughput analysis. We hope that our results may provide guidance for the experimental realization and further investigation of high-performance materials suitable for practical applications. We also suggest that the combination of piezoelectric properties with other characteristic properties of Heuslers, especially magnetic properties, may offer inviting avenues for further development of multifunctional materials.

Acknowledgments

This work was supported in part by ONR Grant N00014-05-1-0054 and N000-14-09-1-0300. Calculations were carried out at the Center for Piezoelectrics by Design. We thank D.R. Hamann, C. Felser, I. Takeuchi, and S.-W. Cheong for useful discussions.

Competing Financial Interests

There are no competing financial interests.

---

[1] H. Nowotny and K. Bachmayer, Monatsch. Chem. **81**, 488 (1950).

[2] A. Belsky, M. Hellenbrandt, V. L. Karen, and P. Luksch,

Acta Cryst. **B58**, 364 (2002).
[3] H. C. Kandpal, C. Felser, and R. Seshadri, J. Phys. D. **39**, 776 (2006).
[4] R. A. deGroot, F. M. Mueller, P. G. vanEngen, and K. H. J. Buschow, Phys. Rev. Lett. **50**, 2024 (1983).
[5] S. Chadov, X. Qi, J. Kubler, G. H. Fecher, C. Felser, and S. C. Zhang, Nature Mater. **9**, 541 (2010).
[6] H. Lin, A. Wray, Y. Xia, S. Xu, S. Jia, R. J. Cava, A. Bansil, and M. Z. Hasan, Nature Mater. **9**, 546 (2010).
[7] C. Felser, G. H. Fecher, and B. Balke, Angew. Chem. Int. Ed. **46**, 668 (2007).
[8] Q. Shen, L. Chen, T. Goto, T. Hirai, J. Yang, G. P. Meisner, and C. Uher, Appl. Phys. Lett. **79**, 4165 (2001).
[9] G. S. Nolas, J. Poon, and M. G. Kanatzidis, MRS Bull. **31**, 199 (2006).
[10] B. Balke, J. Barth, M. Schwall, G. H. Fecher, and C. Felser, J. Elec. Mat. **40**, 702 (2011).
[11] D. M. Wood, A. Zunger, and R. deGroot, Phys. Rev. B. **31**, 2570 (1985).
[12] F. G. Aliev, N. B. Brandt, V. V. Kozyrkov, V. V. Moshchalkov, R. V. Skolozdra, U. V. Stadnik, and V. K. Pecharskii, J. Exp. Theor. Phys. Lett. **45**, 684 (1987).
[13] S. Ogut and K. M. Rabe, Phys. Rev. B. **51**, 10443 (1995).
[14] D. Kieven, R. Lenk, S. Naghavi, C. Felser, and T. Gruhn, Phys. Rev. B. **81**, 075208 (2010).
[15] T. Gruhn, Phys. Rev. B. **82**, 125210 (2010).
[16] F. Casper, R. Seshadri, and C. Felser, Phys. Status Solidi A **206**, 1090 (2009).
[17] K. Kuriyama, K. Nagasawa, and K. Kushida, J. Cryst. Growth **237-239**, 2019 (2002).
[18] K. Kuriyama, K. Kushida, and R. Taguchi, Solid State Comm. **108**, 429 (1998).
[19] X. Gonze, J.-M. Beuken, R. Caracas, F. Detraux, M. Fuchs, G.-M. Rignanese, L. Sindic, M. Verstraete, G. Zerah, F. Jollet, et al., Comp. Mater. Sci. **25**, 478 (2002).
[20] X. Gonze, G. Rignanese, M. Verstraete, J. Beuken, Y. Pouillon, R. Caracas, F. Jollet, M. Torrent, G. Zerah, M. Mikami, et al., Z. Kristall. **220**, 558 (2005).
[21] X. Gonze, B. Amadon, P. Anglade, J. M. Beuken, F. Bottin, P. Boulanger, F. Bruneval, D. Caliste, R. Caracas, M. Cote, et al., Comp. Phys. Comm. **180**, 2582 (2009).
[22] H. J. Monkhorst and J. D. Pack, Phys. Rev. B **13**, 5188 (1976).
[23] A. M. Rappe, K. M. Rabe, E. Kaxiras, and J. D. Joannopoulos, Phys. Rev. B Rapid Comm. **41**, 1227 (1990).
[24] N. J. Ramer and A. M. Rappe, Phys. Rev. B **59**, 12471 (1999).
[25] http://opium.sourceforge.net.
[26] X. Gonze and C. Lee, Phys. Rev. B **55**, 10355 (1997).
[27] M. Born and K. Huang, *Dynamical Theory of Crystal Lattices* (Oxford University Press, Oxford, 1954), we used Eq. (33.28) from this book.
[28] X. Wu, D. Vanderbilt, and D. R. Hamann, Phys. Rev. B **72**, 035105 (2005).
[29] D. R. Hamann, X. Wu, K. M. Rabe, and D. Vanderbilt, Phys. Rev. B **71**, 035117 (2005).
[30] B. B. Karki, G. J. Ackland, and J. Crain, Journal of Physics: Condensed Matter **9**, 8579 (1997).